Science of Sintering, **48** (2016) 221-235

doi: 10.2298/SOS1602221O

UDK 676.017.5; 622.785

Synthesis, Microstructure and Magnetic Properties of Nanocrystalline $MgFe_2O_4$ Particles: Effect of Mixture of Fuels and Sintering Temperature

Ehi-Eromosele Cyril Osereme[1*)], Ita Benedict Iserom[1,2], Iweala Emeka Eze Joshua[3]

[1] Department of Chemistry, Covenant University, PMB 1023, Ota, Nigeria.
[2] Department of Pure and Applied Chemistry, University of Calabar, Calabar, Nigeria.
[3] Department of Biological Sciences, Covenant University, PMB 1023, Ota, Nigeria.

Abstract:

The present article reports the results of studies related to the synthesis of $MgFe_2O_4$ nanocomposite powder by solution combustion process using mixture of fuels containing urea (U) and ammonium acetate (AA). The effect of mixture of fuel and sintering temperature on phase formation, structural, morphological and magnetic properties of $MgFe_2O_4$ particles were investigated by X-ray diffraction (XRD), thermogravimetric analysis (TGA), Raman spectroscopy, scanning electron microscopy (SEM), energy dispersive absorption x-ray (EDAX) and vibrating sample magnetometer (VSM). Thermodynamic modeling of the combustion reaction shows that by using a mixture of urea and ammonium acetate fuels, the adiabatic flame temperature (T_{ad}), exothermicity and amount of gases produced during the combustion process as well as product characteristics could be controlled. The use of mixture of fuels (U and AA) in the synthesis of $MgFe_2O_4$ was found to produce ferrites with finer agglomerates, higher crystallinity, higher magnetic properties and smaller crystallite sizes than when only urea was used. It was found that only samples prepared with a mixture of fuels (0.5U + 0.5AA) and sintered at 900°C for 2 h produced pure ferrite spinel phase while the auto-combusted and powders sintered at 600°C for 2 h had secondary phases. Apart from giving detailed information about the structural order of the samples, Raman spectroscopy also confirmed that $MgFe_2O_4$ is a mixed spinel ferrite.

Keywords: *Solution combustion synthesis; mixture of fuels; sintering temperature; thermodynamic analysis; magnetic nanoparticles.*

1. Introduction

Recently, nanostructures of magnetic materials have received more and more attention due to their unique and novel material properties and their uses in a wide variety of potential applications, such as information storage, cancer therapy, humidity and gas sensing, catalysis, magnetic cell separation and magnetic refrigeration [1-8]. Spinel ferrites with the general formula AFe_2O_4 (A = Mn, Co, Ni, Mg, or Zn) are very important magnetic materials because of their interesting magnetic and electrical properties with chemical and thermal stabilities [9]. Amongst the spinel ferrite families, magnesium ferrite ($MgFe_2O_4$) is a soft

*) **Corresponding author**: cyril.ehi-eromosele@covenantuniversity.edu.ng

magnetic n-type semi-conducting material [10] which finds applications in the fields of heterogeneous catalysis, adsorption, sensors and magnetic technologies [11].

It is well known that most of the physical and chemical properties which determines the applicability of spinel ferrites depends on the shape and size of nanoparticles and the thermal history of sample preparation as well [12-16]. Therefore, the synthesis method plays a very important role on the physical, chemical, structural, and magnetic properties of a spinel ferrite. Various methods of synthesis such as ball milling [17-19], co-precipitation [20-22], sol-gel [21, 23], reverse micelle [22, 24], hydrothermal [25] and combustion methods have been used for the synthesis of $MgFe_2O_4$ nanoparticles. The spinel ferrite particles synthesized by solid-state methods show an assembly of irregular shapes and agglomerations [26] while those prepared by most wet chemical methods require careful control of pH of the solution, temperature and concentration like parameters for formation of particles. So among the various methods for synthesizing ferrites, the combustion method stands out as an alternative and highly promising method [27]. Combustion method offers low processing time, relatively lower operating-temperature and cost effectiveness in the synthesis of ferrites. Furthermore, combustion method imparts significant advantages like good stoichiometric control and ultrafine particle formation with narrow size distribution, which has an important influence on the magnetic properties of the ferrite [4, 28-30].

Although $MgFe_2O_4$, like many other ferrites, is routinely synthesized by combustion method using glycine as fuel [14, 31]; other fuels like polyvinyl alcohol [32], citric acid [4, 22, 33] and urea [21] have also been used. The powder characteristics such as crystallite size, surface area, size distribution and nature of agglomeration are primarily governed by enthalpy or flame temperature generated during combustion which itself is dependent on the nature of the fuel. In combustion synthesis, among various control parameters in a combustion process, fuel plays an important role in determining the morphology, phase, and particulate properties of the final product [28]. Therefore, studies pertaining to the effect of fuel on the structural, morphological and magnetic properties of ferrites are important in understanding their inter-relationships and establishing the effect of different fuels on their properties hence, they need to be explored.

It has been reported that using urea as a fuel yields powders with low specific surface area and hard agglomerates, because of the formation of sTab. polymeric intermediates that prevent the dissipation of heat and thereby sintering the oxides during combustion [34]. So a mixture of fuels with different exothermicity has been used here. To the best of our knowledge, a mixture of urea and ammonium acetate fuels in the combustion synthesis of $MgFe_2O_4$ has not yet been reported. Thus, in the present work, we report the synthesis of $MgFe_2O_4$ particles using a mixture of urea and ammonium acetate. Then the as-prepared (auto-combusted) powders were annealed at 600°C and 900°C for 2 hours in air. The effect of mixture of fuel and sintering temperature on phase formation, structural, morphological and magnetic properties of $MgFe_2O_4$ particles were studied.

2. Experimental

2.1 Materials

Analytical grade $Mg(NO_3)6H_2O$ (99% purity of Alfar Aesar), $Fe(NO_3)_3.9H_2O$ (99% purity of Sigma Aldrich), urea (U, CH_4N_2O) and ammonium acetate (AA, CH_3COONH_4) obtained from SD Fine Chem. Ltd., Mumbai were used as starting materials.

2.2 Experimental Method

First, to prepare $MgFe_2O_4$-I, 5.1282 g $Mg(NO_3)_2.6H_2O$, 16.16 g $Fe(NO_3)_3.9H_2O$ and 8.012 g of urea were dissolved in 20 ml of de-ionised water. Then the solutions were heated

to 80°C to form a viscuous gel of precursors under magnetic stirring. Secondly, the gel is transferred to a pre-heated coil (300°C). Finally, after a short moment, the solution precursors boiled, swelled, evolved a large amount of gases and ignited, followed by the yielding of puffy black products. Part of this final product (auto-combustion powder) was annealed at 600°C and another part annealed at 900°C for 2h each. Similarly, $MgFe_2O_4$-II was prepared following the same procedures used in $MgFe_2O_4$-I except that 4.006 g urea and 2.806 g ammonium acetate were used while in the preparation of $MgFe_2O_4$-III, 6.01 g urea and 1.404 g ammonium acetate were used. In the preparation of $MgFe_2O_4$-II, the stoichiometric amount of urea (U) calculated was not used instead, 0.5 times the stoichiometric value (0.5U) was used, i.e., instead of 8.012 g urea, 4.006 g urea was used (for 5.1282 g $Mg(NO_3)_2.6H_2O$ and 16.16 g $Fe(NO_3)_3.9H_2O$). To compensate the fuel ratio, extra fuel ammonium acetate was used. Similarly, instead of 5.616 g of ammonium acetate (AA), 2.806 g [0.5 times the stoichiometric value (0.5AA)] was used. For $MgFe_2O_4$-III, similar calculations were carried out using 6.01 g (0.75U) instead of 8.012 g and 1.404 g of ammonium acetate (0.25 AA) was used instead of 5.616 g of ammonium acetate. In all cases, the molar ratio of metal nitrates to the mixture of urea and ammonium acetate was stoichiometric. The stoichiometric amount of the corresponding metal nitrates was acting as an oxidizing agent and the fuel (urea and ammonium acetate) as the reducing agent for the combustion reaction.

2.3 Characterisation Methods

TGA of precursor materials was carried out in a temperature range of 30-1000°C in air atmosphere with a heating rate of 10°C/min, to study the thermal evolution of the precursors to monitor the combustion process using STA 409 PC Luxx from NETZSCH-Geratebau (Germany). The X-ray diffractograms of the auto-combustion and annealed powders were recorded using an X-ray diffractometer (D8 Advance, Brucker, Germany), equipped with a Cu Kα radiation source (λ = 1.5406 A°) and the crystallite size is calculated by the well-known Debye-Scherrer relation. The surface morphology and elemental detection were examined with a scanning electron microscope (SEM) Ametek model XL30 Lab 6. Magnetic measurements were carried out with a vibrating sample magnetometer (VSM, Lake Shore cryotronics-7400 series) at room temperature. The Raman measurement was carried out at room tempearture with an Olympus BX41 (Hariba Jobin–Yvon) Raman microscope equipped with a He–Ne laser of 633 nm as an excitation source and an optical microscope with 50× objective. The magnetic characterizations were carried out with a Vibrating Scanning Magnetometer (Lake Shore cryotronics-7400 series) under the applied field of ±20,000 G at room temperature.

3. Results and Discussion

3.1 Combustion Reaction and Thermodynamic Analysis

The theoretical stoichiometric equations for the formation of $MgFe_2O_4$-I (Eq. 1), $MgFe_2O_4$-II (Eq. 2) and $MgFe_2O_4$-III (Eq. 3) can be written as follows:

$$Mg(NO_3)_2.6H_2O + 2Fe(NO_3)_3.9H_2O + 6.67CH_4N_2O + (9.99 - 10)O_2 \rightarrow \mathbf{MgFe_2O_4\text{-}I} + 6.67CO_2\uparrow + 37.33H_2O\uparrow + 10.67N_2\uparrow \quad (1)$$

$$Mg(NO_3)_2.6H_2O + 2Fe(NO_3)_3.9H_2O + 3.34CH_4N_2O + 1.82CH_3COONH_4 + (9.99 - 10)O_2 \rightarrow \mathbf{MgFe_2O_4\text{-}II} + 6.98CO_2\uparrow + 34.32H_2O\uparrow + 8.25N_2\uparrow \quad (2)$$

$$Mg(NO_3)_2.6H_2O + 2Fe(NO_3)_3.9H_2O + 5.00CH_4N_2O + 0.91CH_3COONH_4 + (9.99 - 10)O_2 \rightarrow \mathbf{MgFe_2O_4\text{-}III} + 6.82CO_2\uparrow + 35.83H_2O\uparrow + 5.46N_2\uparrow \quad (3)$$

For $MgFe_2O_4$-I, the precursor mixture was yellowish and the combustion type was smouldering combustion with lots of smoke. For $MgFe_2O_4$-II (0.5U + 0.5AA) and $MgFe_2O_4$-III (0.75U + 0.25AA), the precursor mixtures were red (apparently due to the ammonium

acetate introduced) and the combustion type was smouldering combustion with less smoke for $MgFe_2O_4$-II and flamy combustion for $MgFe_2O_4$-III. In all three different samples, combusted products resulted in a mixture of coarsely formed brownish powders.

The theoretical calculations based on thermodynamic consideration such as enthalpy of reaction and flame temperature helps in estimation of exact ignition condition and to predict the exothermicity of the different fuel mixture used. Enthalpy of reaction depends on the heat of formation of products and reactants [14]. The following equation is used to calculate the enthalpy of reaction:

$$\Delta H^{O} = \left(\sum n\Delta H_f^{O}\right)_{products} - \left(\sum n\Delta H_f^{O}\right)_{reactants} \quad (4)$$

where n is the number of moles, ΔH_f^{O} is heat of formation and ΔH^{O} is enthalpy of reaction.

The thermodynamic data for the various reactants and products involved in the combustion reaction are given in Tab. I. The enthalpy of reaction for the formation of $MgFe_2O_4$-I, $MgFe_2O_4$-II and $MgFe_2O_4$-III samples can be calculated by using the thermodynamic data (Tab. I) and Eqs. 1-3. The enthalpy of reaction for the formation of $MgFe_2O_4$-I, $MgFe_2O_4$-II and $MgFe_2O_4$-III samples were −377.91 kcal mol^{-1}, −242.97 kcal mol^{-1} and −310.61 kcal mol^{-1}, respectively. The results show that urea ($MgFe_2O_4$-I) had the highest exothermicity while 0.5U + 0.5AA fuel mixture ($MgFe_2O_4$-II) had the lowest.

Tab. I Standard thermodynamic data for the reactants and products of the combustion reaction [14, 36]

Compound	Heat of formation, ΔH_f^{O} (kcal/mol)	Heat capacities, C_p (cal mol^{-1} K^{-1})
$Fe(NO_3)_3.9H_2O$ (s)	−785.2	–
$Mg(NO_3)_2.6H_2O$ (s)	−624.48	–
CH_4N_2O (s)	−83.28	–
CH_3COONH_4 (s)	−147	–
H_2O (g)	−57.79	7.2 + 0.0036 T
CO_2 (g)	−94.05	10.34 + 0.00274 T
N_2 (g)	0	6.5 + 0.001 T
O_2 (g)	0	5.92 + 0.00367 T
$MgFe_2O_4$ (s)	−343.69	34.16

All values considered at standard temperature T= 298 K.

Tab. II Effect of mixture of fuels on adiabatic flame temperature (T_{ad}), heat absorbed (Q) by product and number of moles of gases evolved during combustion

Sample	Mixture of fuel	Q, (kcal mol^{-1})	T_{ad} (K)	Amount of gases produced during combustion (moles)
$MgFe_2O_4$-I	U	377.91	1158	54.7
$MgFe_2O_4$-II	0.5U + 0.5AA	242.97	831	49.6
$MgFe_2O_4$-III	0.75U + 0.25AA	310.61	995	48.1

The heat absorbed by product during combustion reaction can be theoretically approximated as:

$$Q = -\Delta H^{O} = \int_{298}^{T_{ad}} \left(\sum nC_P\right)_{products} dT \quad (5)$$

Eq. (5) can be modified to calculate adiabatic flame temperature (T_{ad}) as follows [14]:

$$T_{ad} = T + \frac{Q}{C_P} \quad (6)$$

where Q is the heat absorbed by products under adiabatic condition, T is the reference temperature (T= 298 K) and C_p is the heat capacity of the products at constant pressure. Using the values for the enthalpy of reaction for the formation of $MgFe_2O_4$-I, $MgFe_2O_4$-II and $MgFe_2O_4$-III samples, data from Tab. I and Eqs. 5 and 6; the adiabatic flame temperatures and heat absorbed by the products, prepared by using only urea ($MgFe_2O_4$-I) and a mixture of urea and ammonium acetate ($MgFe_2O_4$-II and $MgFe_2O_4$-III) as fuels, were calculated and given in Tab. II. The values of the theoretically calculated T_{ad} and Q decreased with decreasing amount of urea used with $MgFe_2O_4$-II sample recording the lowest values. The reaction temperature and T_{ad} increase with increase in the amount of urea. The amount of gases evolved also followed the same trend except that there was a higher evolution of gases in the formation of $MgFe_2O_4$-II compared with the $MgFe_2O_4$-III sample. This is due to the higher amount of AA used in the synthesis of $MgFe_2O_4$-II. Experimentally, it has been observed that fuel mixture combination reaction not only reduces the intensity of the combustion reaction it also reduces the particle size of as-synthesized powder [35]. So, ammonium acetate has been used to reduce the exothermicity of urea which might also impact on the structural, morphological and magnetic properties of the sample.

3.2. TG Analysis

TGA was used to study the thermal evolution of the precursors to monitor the combustion process. Fig. 1 shows the TGA plots for the precursor gels for the combustion synthesis of $MgFe_2O_4$ samples (I-III). The pyrolysis reaction of urea in an open reaction vessel can be divided into three major reaction regions. These regions are dominated by different chemical processes associated with the mass loss stages observed in the TGA [37]. The TGA results show three decomposition steps in $MgFe_2O_4$-I sample but four decomposition steps in $MgFe_2O_4$-II and $MgFe_2O_4$-III samples. The fourth decomposition step occurring at 275-375^{o}C (~10% weight loss) for $MgFe_2O_4$-II and 290-350^{o}C (~7% weight loss) for $MgFe_2O_4$-III might be due to the decomposition of unreacted ammonium acetate that was absent in $MgFe_2O_4$-I sample. The increased weight loss for $MgFe_2O_4$-II compared with $MgFe_2O_4$-III might be due to the amounts of ammonium acetate added in the precursors with $MgFe_2O_4$-II having a higher amount. The first decomposition step in the $MgFe_2O_4$-I (~30-135^{o}C), $MgFe_2O_4$-II (~30-150^{o}C) and $MgFe_2O_4$-III (~30-165^{o}C) curves show a weight loss of 18%, 32% and 23%, respectively. This was attributed to complete evaporation of water and organic content in the precursor gels. The weight loss corresponds to the amount of organic content in the precursor gels with $MgFe_2O_4$-II having the highest and $MgFe_2O_4$-I having the lowest. The second decomposition step in the $MgFe_2O_4$-I (~135-220^{o}C), $MgFe_2O_4$-II (~150-220^{o}C) and $MgFe_2O_4$-III (~165-230^{o}C) curves shows a weight loss of 26%, 8% and 20%, respectively. Chen and Isa [38] reported that biuret, a product of urea decomposition, decomposes corresponding to the second step. Here, the weight loss corresponds to the amount of urea in the precursor gels with $MgFe_2O_4$-I recording the highest and $MgFe_2O_4$-II recording the lowest. The third decomposition step for $MgFe_2O_4$-I (~220-300^{o}C), $MgFe_2O_4$-II (~220-280^{o}C) and $MgFe_2O_4$-III (~230-300^{o}C) curves shows a weight loss of 32%, 30% and 25%, respectively. This indicates the occurrence of combustion reaction during the decomposition of nitrate-fuel (urea and ammonium acetate) dried gel thereby recording the highest weight loss of all decomposition steps. These results are consistent with the reaction conditions.

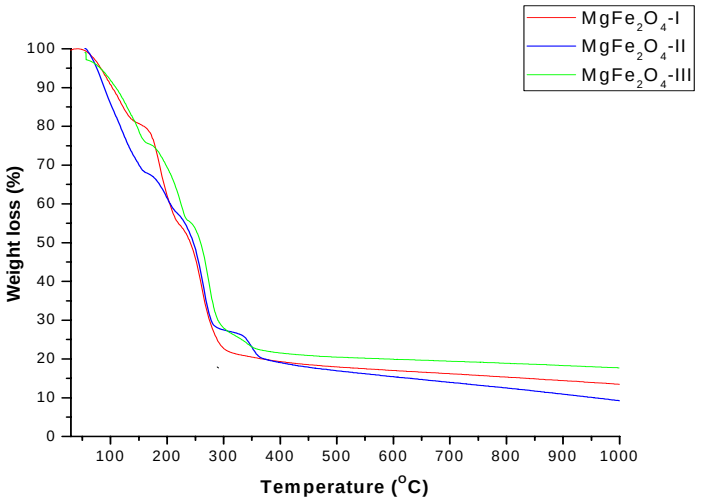

Fig. 1. TGA curves of the precursors gels for $MgFe_2O_4$ I-III samples.

3.3. Structural and Phase Analysis

The crystallinity and structural properties of $MgFe_2O_4$ samples prepared using a mixture of fuel approach and annealed at 900°C for 2h were studied by X-ray diffractometer and the patterns are shown in Fig. 2. X-ray diffraction patterns of $MgFe_2O_4$ samples annealed at 600°C for 2hrs is shown in Fig. 3. The estimated values of the effect of using both urea and a mixture of fuels on the structural parameters of $MgFe_2O_4$ MNPs annealed at 900°C for 2h are given in Tab. III. The obtained peaks are well matched to the cubic spinel structure with standard JCPDS card no. 73-1720 files for $MgFe_2O_4$. The XRD lines are presented with miller indices. As shown in Fig. 2, spinel ferrite crystallises completely only after annealing at 900°C for 2hrs; however, only $MgFe_2O_4$-II sample (0.5U + 0.5AA) obtained a pure $MgFe_2O_4$ phase while $MgFe_2O_4$-I and $MgFe_2O_4$-II samples had a secondary haematite (α-Fe_2O_3) phase (JCPDS card no. 33-0664) present with the spinel phase. Fig. 3 shows that impure XRD reflections, which is due to the presence of haematite phase are present after annealing at 600°C for 2h and only disappears after annealing at 900°C for 2h. Conventionally, sintering temperature of $MgFe_2O_4$ is very high [39]. Therefore, it remains difficult to synthesise phase pure $MgFe_2O_4$ spinels especially at low calcinations temperature [40]. Also, iron oxide is known to co-exist with desired cubic spinel phase of $MgFe_2O_4$ [41]. The XRD patterns for the auto-combustion powders for all samples were poor crystalline (XRD patterns not included). The results indicate that a single cubic spinel $MgFe_2O_4$ phase can only be obtained by using a combination of urea and ammonium acetate (0.5U+0.5AA) fuels with annealing at 900°C for 2h in the solution combustion synthesis of $MgFe_2O_4$.

XRD data enables the investigation of the role of using both urea and a mixture of fuel in modifying the structural parameters such as crystallite size (D), lattice constant (a), X-ray density (D_x) and unit cell volume (V) for synthesized $MgFe_2O_4$. From the XRD data, D of the annealed samples was calculated using the Scherrer Equation [28]:

$$D = \frac{0.9\lambda}{\beta Cos\theta} \quad (4)$$

where, β is breadth of the observed diffraction line at its half intensity maximum, K is the so-called shape factor, which usually takes a value of about 0.9 and λ is the wavelength of the X-ray source used in XRD. It can be seen from Tab. III that the values of D, a and V decreases from using only urea to using a combination of fuels with $MgFe_2O_4$-III (0.75U+0.25AA) having the lowest values of these parameters. Conversely, X-ray density is found to increase

from using only urea to using a combination of fuels with $MgFe_2O_4$-III having the highest value. As stated earlier, using urea alone as a fuel leads to the formation of hard agglomerates. As observed in the synthesis of $MgFe_2O_4$-I, it was a smouldering combustion with lots of smoke which might have resulted to sintering the oxides hence, it has the highest values of D, a and V parameters. With the addition of ammonium acetate, the smouldering combustion changed to flamy one in $MgFe_2O_4$-III and combustion process was faster resulting in the lower values of these parameters. The observed decrease in density of the powders from samples $MgFe_2O_4$-III to $MgFe_2O_4$-I could be attributed to reduction of oxygen vacancies which play a predominant role in accelerating densification, i.e. the decrease in oxygen ion diffusion would retard the densification [42]. This decrease in oxygen ion diffusion might have resulted due to the smouldering combustion seen in $MgFe_2O_4$-I sample thereby showing the lowest density.

Tab. III Effect of using both urea and a mixture of fuel on the structural properties of $MgFe_2O_4$ nanoparticles annealed at 900°C

Fuel	Crystallite size, D, (nm)	Lattice constant, a, (nm)	Unit cell volume, V, nm^3	X-ray density, D_x, g/cm^3
Urea (U/N = 2.22)	59	0.839	0.5906	4.4985
Urea (0.5) + AA (0.5)	53	0.838	0.5885	4.5147
Urea (0.75) + AA (0.25)	47	0.837	0.5864	4.5309

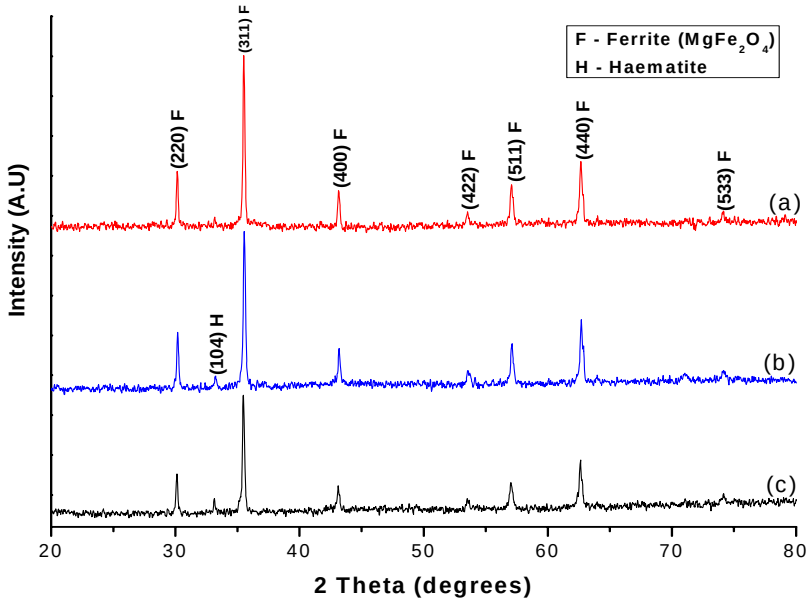

Fig. 2. XRD patterns of $MgFe_2O_4$ sample annealed at 900°C for 2h: (a) $MgFe_2O_4$-II (b) $MgFe_2O_4$-III (c) $MgFe_2O_4$-I.

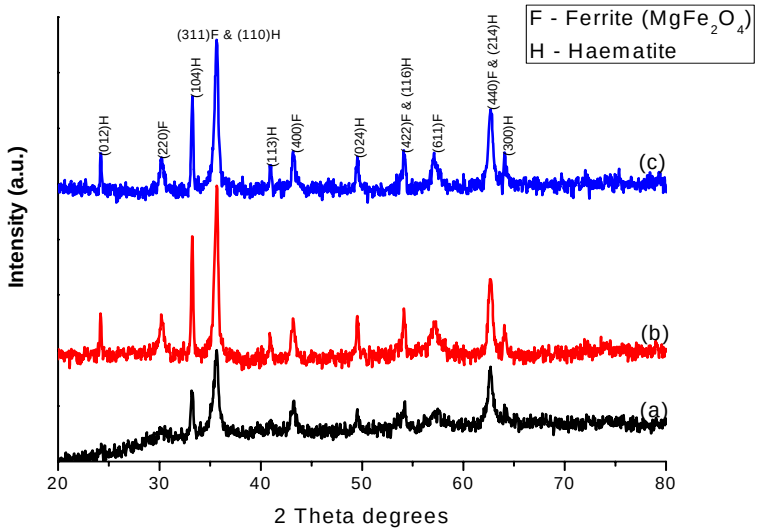

Fig. 3. XRD patterns of $MgFe_2O_4$ sample annealed at 600°C for 2h: (a) $MgFe_2O_4$-II (b) $MgFe_2O_4$-III (c) $MgFe_2O_4$-I.

3.4. Raman Studies

Room temperature Raman spectra of samples prepared using a mixture of fuel approach and annealed at 900°C for 2hrs were recorded in the range of 0–1000 cm^{-1}, as shown in Fig. 4. Raman spectroscopy is one powerful technique to study the microstructure of crystalline compounds. The Raman features are assigned to the vibrational modes from the nanoparticles crystalline structure. $MgFe_2O_4$ crystallizes in a spinel structure of space group *Fd*-3*m* and group theoretical calculations results in five Raman active bands namely $A_{1g} + E_g + 3F_{2g}$ [43]. The five Raman modes are all observed in the three samples but $MgFe_2O_4$-I gave other peaks at 290, 405 and 610 cm^{-1} which were assigned to E_g modes of α-Fe_2O_3 [44].

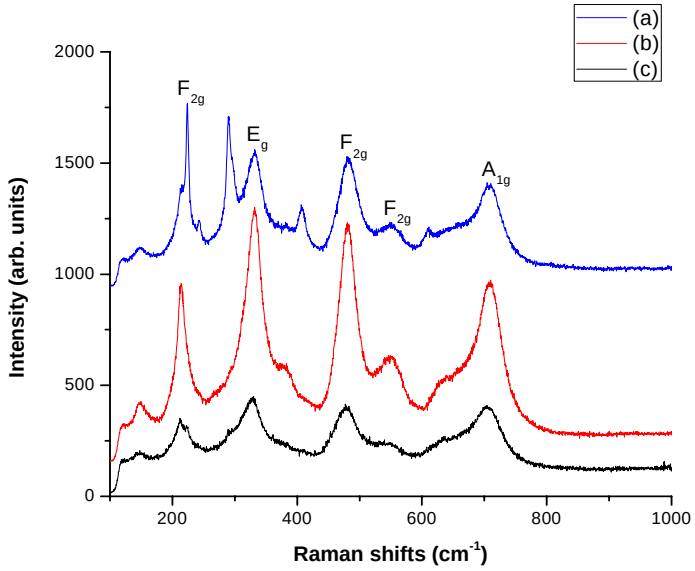

Fig. 4. Raman spectrum of $MgFe_2O_4$ samples synthesised using a mixture of fuel approach and sintered at 900°C for 2h: (a) $MgFe_2O_4$-II (b) $MgFe_2O_4$-III (c) $MgFe_2O_4$-I.

This results are consistent with the presence of α-Fe_2O_3 phase in the XRD of $MgFe_2O_4$-I but surprisingly these modes were absent in $MgFe_2O_4$-III sample which also showed α-Fe_2O_3 phase in its XRD. $MgFe_2O_4$-II sample shows a broad Raman mode at 635 cm^{-1} which is also present in $MgFe_2O_4$-I sample. This mode has both been attributed to order-disorder effect [45] and the substitution of the Fe^{3+} ions by Mg^{2+} ions in the tetrahedral sites [46]. The Raman modes of $MgFe_2O_4$-II are the sharpest of the three samples and are well defined. From the Raman spectrum, it is very probable that the local structure of $MgFe_2O_4$-II is different from the other samples. The A_{1g} mode is due to symmetric stretching of oxygen atoms along Fe-O (and Mg-O) bonds in the tetrahedral coordination. E_g is due to symmetric bending of oxygen with respect to the metal ion and $F_{2g(3)}$ is caused by asymmetric bending of oxygen. $F_{2g(2)}$ is due to asymmetric stretching of Fe (Mg) and O. $F_{2g(2)}$ and $F_{2g(3)}$ correspond to the vibrations of octahedral group. $F_{2g(1)}$ is due to translational movement of the tetrahedron (metal ion at tetrahedral site together with four oxygen atoms) [47]. The results from the Raman studies show that the samples prepared are spinel in structure and confirms that $MgFe_2O_4$ is a mixed spinel.

3.5. Morphological and Chemical Composition Analysis

The SEM micrographs of samples annealed at 900^{o}C for 2 h were obtained to study the morphology and microstructure and are shown in Figs 5a-c. For all the samples, the micrographs showed remarkable changes in microstructure regarding the level of agglomeration and particle distribution by using both urea and a mixture of fuel. Fig 5a showed the highest agglomeration of all samples with Fig. 5c having the least agglomerates with smaller particle size distribution (which might be due to the flamy combustion) confirming the values of crystallite sizes calculated from XRD results. The urea process yields oxides of high agglomerates. The use of mixture of fuels concept allows for the tunability of the crystallite sizes and agglomeration of nanoparticles. The images also showed a faceted and irregular morphology in Fig. 5a (only urea) to a faceted and fairly regular shape in Fig. 5c (0.75U+0.25AA). The results reveal that the particles morphologies and sizes are dependent on the chemical composition of the fuel used in the combustion process; and the addition of ammonium acetate to fuel (urea) causes a better combustion with the production of finer agglomerates.

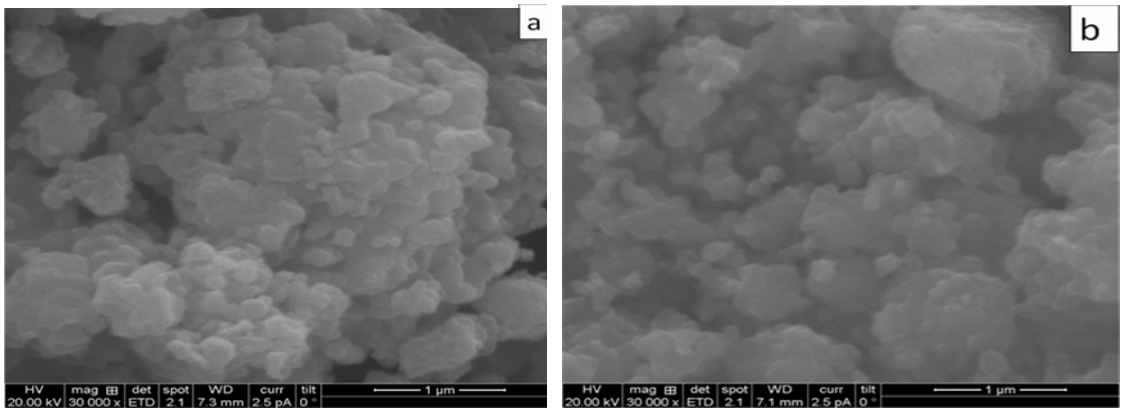

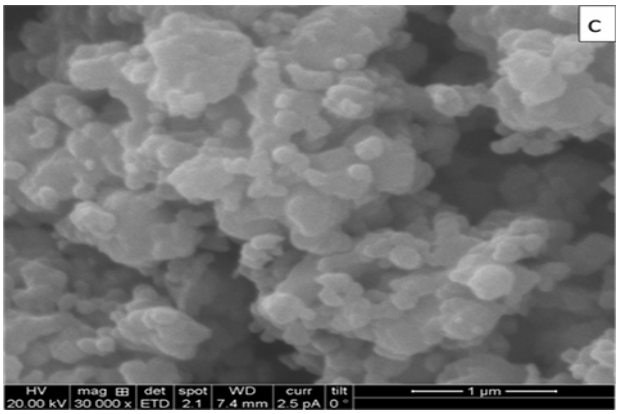

Fig. 5. SEM micrographs of $MgFe_2O_4$ MNPs using both urea and a mixture of fuel and annealed at 900°C for 2 h (a) $MgFe_2O_4$-I (b) $MgFe_2O_4$-II (c) $MgFe_2O_4$-III.

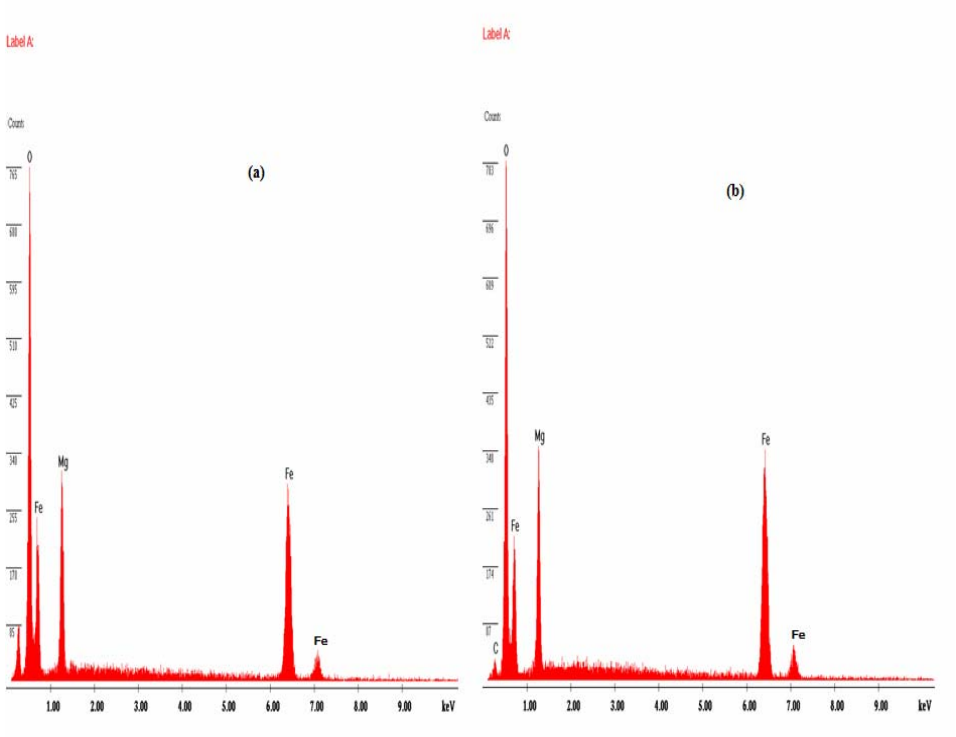

Fig. 6. EDAX spectra obtained using both urea and a mixture of fuel and annealed at 900°C for 2 h (a) $MgFe_2O_4$-I (b) $MgFe_2O_4$-II.

EDAX analysis was used to investigate the chemical composition for the constituent elements of the synthesised MNPs. The EDAX spectra for $MgFe_2O_4$-I and $MgFe_2O_4$-II are shown in Figs. 6a-b, respectively. The EDAX results showed that the products did not contain any impurity elements, and the compositional molar ratio of Mg to Fe for $MgFe_2O_4$-II (Mg = 14.20%, Fe = 30.52%, O = 55.40%) was closer to 0.5 than $MgFe_2O_4$-I (Mg = 13.88%, Fe = 30.53%, O = 53.20%) which also had less oxygen (a factor that might have accounted for the decrease in the density of the powders shown by XRD analysis).

3.6. Magnetic Studies

The specific magnetization curves of $MgFe_2O_4$ samples annealed at 900°C and 600°C for 2 h, obtained from room temperature VSM measurements are shown in Fig. 7. and Fig. 8,

respectively. The effect of heat treatment and the use of both urea and a mixture of fuel on the magnetic properties are given in Tab. IV. $MgFe_2O_4$ is a mixed type spinel ferrite with the Mg^{2+} and Fe^{3+} metal ions distributed over the tetrahedral and octahedral sites. Among the various ferrites, $MgFe_2O_4$ is an interesting magnetic material where magnetic couplings purely originate from the magnetic moment of Fe cations and may be relatively weaker due to non magnetic Mg^{2+} metal ions [14]. Figs. 7 and 8 show curves that are typical of a soft magnetic material and indicate hysteresis loops. From these measurements, saturation magnetization (M_s), remanent magnetization (M_r), coercivity (H_c) and loop squareness ratio (M_r/M_s) were derived and listed in Tab. IV. For all samples except for the H_c values of $MgFe_2O_4$-III, the magnetic properties values were lesser for the samples annealed at 600°C than 900°C. This can be attributed to the impure secondary phase (α-Fe_2O_3) present in their XRD patterns after annealing at 600°C for 2 h. It can also be seen that the M_s, M_r, H_c and M_r/M_s values for $MgFe_2O_4$-I sample are the least as compared to other samples. This is attributed to the poor crystallization of the $MgFe_2O_4$ phase in both heat treated samples. $MgFe_2O_4$-II sample annealed at 900°C recorded the highest M_s, M_r, H_c and M_r/M_s values of all samples. These can be attributed to its pure crystalline $MgFe_2O_4$ phase. It recorded an M_s of 26 emu/g which is close to that of the bulk $MgFe_2O_4$ material (~30 emu/g) [48]. The M_s of the NPs were less than the corresponding bulk value. This reduced magnetization of nanosized magnetic particles is explained by the surface spin disorder which is due to cation redistribution or the formation of spin glass like structure in the near-surface layers [49, 50]. The presence of canted antiferromagnetic α-Fe_2O_3, may have contributed to the reduction in the magnetization of $MgFe_2O_4$-I and $MgFe_2O_4$-III samples annealed at 900°C. The loop squareness ratio (M_r/M_s) is found to be around 0.5 for all samples which is the expected value for randomly packed single domain particles. Clearly, the magnetic properties of $MgFe_2O_4$ MNPs show a dependence on the type of fuel and the heat treatment.

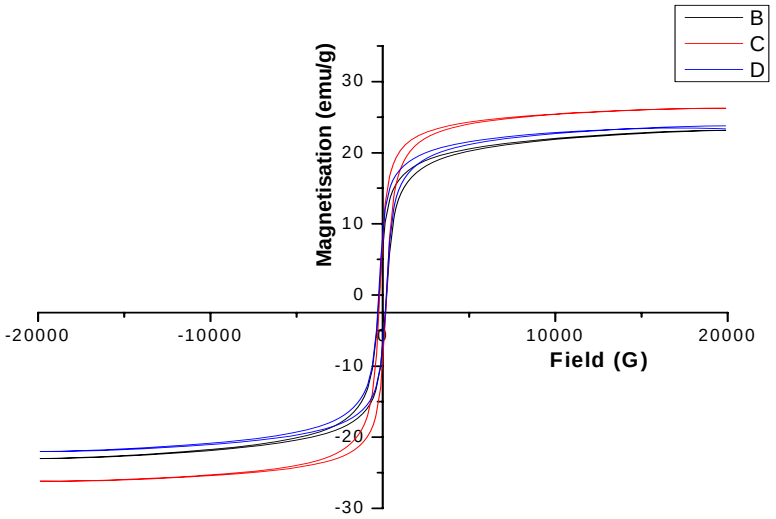

Fig. 7. Magnetic hysteresis curves (measured at room temperature) of $MgFe_2O_4$ synthesised using a mixture of fuel approach and sintered at 900°C for 2 h: (a) $MgFe_2O_4$-I [using only urea (U/N = 2.22)], (b) $MgFe_2O_4$-II (0.5U + 0.5AA) and (c) $MgFe_2O_4$-III (0.75U + 0.25AA).

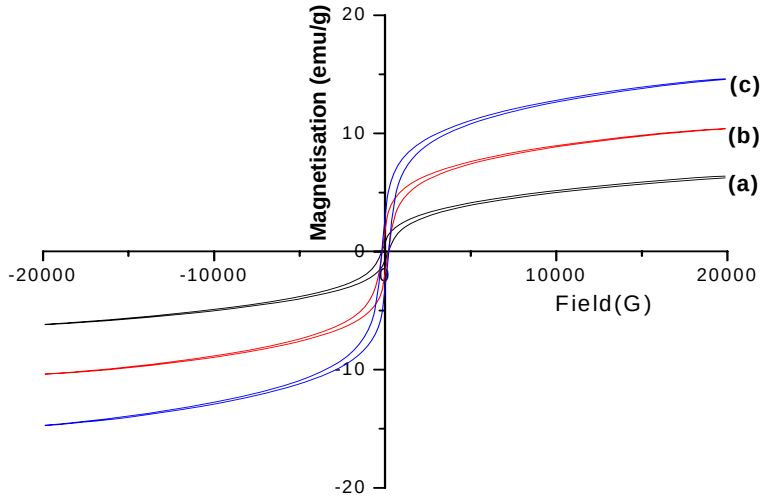

Fig. 8. Magnetic hysteresis curves (measured at room temperature) of $MgFe_2O_4$ synthesised using a mixture of fuel approach and sintered at 600°C for 2 h: (a) $MgFe_2O_4$-I [using only urea (U/N = 2.22)], (b) $MgFe_2O_4$-II (0.5U + 0.5AA) and (c) $MgFe_2O_4$-III (0.75U + 0.25AA)

4. Conclusion

The solution combustion synthesis of $MgFe_2O_4$ using a mixture of fuels and the effect of sintering temperature on the phase formation, structure, morphological and magnetic properties has been studied. A thermodynamic consideration of the combustion reaction shows that the adiabatic flame temperature, exothermicity and the amount of gas produced decreased with decrease in the amounts of urea. These were also found to control the product characteristics. Addition of ammonium acetate markedly altered the combustion type from smouldering combustion with lots of smoke to flame combustion with lesser generation of smoke depending on the amount of ammonium acetate added. The crystallite size and other structural properties (lattice constant and unit cell volume) were higher in the sample synthesized with only urea than when mixtures of fuels were used. The results from the combustion reaction indicate that a single cubic spinel $MgFe_2O_4$ phase was only obtained when a combination of urea and ammonium acetate (0.5U + 0.5AA) fuels was used in the solution combustion synthesis of $MgFe_2O_4$ with annealing at 900°C for 2h. The samples prepared with the mixture of fuels were found to produce ferrites with finer agglomerates than when only urea was used. Also, it was established that the magnetic properties of $MgFe_2O_4$ MNPs synthesized with a mixture of fuel and those sintered at 900°C for 2h presented higher magnetic properties than samples synthesized with only urea and those sintered at 600°C for 2 hrs. Raman spectroscopy also gave detailed information about the structural order of the samples. In all, only $MgFe_2O_4$ sample synthesized with a mixture of fuel (0.5U + 0.5AA) and sintered at 900°C for 2h had the pure spinel ferrite phase and the highest saturation magnetization (26 emu/g) which is close to that of the bulk $MgFe_2O_4$.

Acknowledgements

This work would not have been possible without the visiting research grant given to Mr. Ehi-Eromosele C.O. by the International Centre for Materials Science, Jawarharlal Nehru Centre for Advanced Scientific Research, Bangalore, India. The authors would like to thank the Department of Materials Engineering, India Institute of Science, Bangalore, India for

providing TGA and VSM facilities. We also like to thank Professor Chandra Srivastava and his student, Mr. Mahander Singh for helping with the VSM analysis.

5. References

1. S. Maensiri, M. Sangmanee, W. Wiengmoon, Nanoscale Res Lett., 4 (2009) 221–228.
2. S. A. Hosseini, D. Salari, A. Niaei, F. Deganello, G. Pantaleo, P. Hojati, Journal of Environmental Science and Health, Part A, 46:3 (2011), 291-297.
3. S. Kanagesan, M. Hashim, S. Tamilselvan, N. B. Alitheen, I. Ismail, G. Bahmanrokh, Journal of Nanomaterials, (2013) 1-8.
4. J. Y. Patil, I. S. Mulla, S. S. Suryavanshi, Materials Research Bulletin, 48 (2013) 778–784.
5. I. K. Bajpai, Balani, B. Basu, J. Am. Ceram. Soc., 96 (7) (2013) 2100–2108.
6. N. D. Thorat, S. V. Otari, R. A. Bohara, H. M. Yadav, V. M. Khot, A. B. Salunkhe, M. R. Phdatre, A. I. Prasad, R. S. Ningthoujam, S. H. Pawar, Materials Science and Engineering C 42 (2014) 637-646.
7. P. A. Liberti, C. G. Rao, L. Terstappen, Journal of Magnetism and Magnetic Materials, 225(1-2) (2001) 301-307.
8. N. Kasapoglu, B. Birsoz, A. Baykal, Cent. Eur. J. Chem., 5 (2007) 570–580.
9. R. Valenzuela, Magnetic Ceramics, Cambridge University Press, Cambridge, 1994.
10. N. Sivakumar, A. Narayanasamy, J. -M. Greneche, R. Murugaraj, Y. S. Lee, Journal of Alloys and Compounds, 504(2) (2010) 395–402.
11. S. V. Bangale, D. R. Patil, S. R. Bamane, Arch. Appl. Sci. Res., 3 (5) (2011) 506–513.
12. A. Franco Jr., T. E. Pereira Alves, E. C. de Oliveira Lima, E. da Silva Nunes, V. Zapf, Appl Phys A., 94 (2009) 131–137.
13. S. Ayyappan, J. Philip, B. Raj, Mater. Chem. Phys., 115 (2009) 712-717.
14. V. M. Khot, A. B. Salunkhe, M. R. Phadatare, S. H. Pawar, Materials Chemistry and Physics, 132 (2012) 782–787.
15. A. Franco Jr., V. Zapf, J. Magn. Magn. Mater., 320 (5) (2008) 709-713.
16. D. R. Cornejo, A. Medina-Boudri, H. R. Bertorello, J. Matutes Aquino, J. Magn. Magn. Mater., 242 (2002) 194.
17. M. Rabanal, A. Várez, B. Levenfeld, J. Torralba, J. Mater. Process. Technol., 143 (2003) 470-474.
18. M. Gateshki, V. Petkov, S. K. Pradhan, T. Vogt, J. Appl. Cryst., 38 (2005) 772–779.
19. N. Sivakumar, A. Narayanasamy, J. -M. Greneche, R. Murugaraj, Y. S. Lee, J. Alloys Compd., 504 (2010) 395-402.
20. Q. Chen, A. J. Rondinone, B. C. Chakoumakos, Z. John Zhang, Journal of Magnetism and Magnetic Materials, 194(1) (1999) 1–7.
21. N. Kaur, M. Kaur, Processing and Application of Ceramics, 8(3) (2014) 137–143.
22. J. Chandradass, A. H. Jadhav, K. H. Kim, H. Kim, Journal of Alloys and Compounds, 517 (2012) 164–169.
23. L. J. Berchmans, R. K. Selvan, P. N. S. Kumar, C. O. Augustin, J. Magn. Magn. Mater., 279 (2004) 103-110.
24. P. Holec, J. Plocek, D. Niznansky, J. Poltierova Vejpravov, J. Sol–Gel Sci. Technol., 51(3) (2009) 301-305.
25. T. Sasakia, S. Oharaa, T. Nakaa, J. Vejpravovab, V. Sechovskyb, M. Umetsua, S. Takamia, B. Jeyadevanc, T. Adschiria, J. Supercrit. Fluids, 53(3) (2010) 92-94.
26. H. Deng, H. Chen, H. Li, Materials Chemistry and Physics, 101(2-3) (2007) 509–513.
27. A. C. M. Costa, E. Tortella, M. R. Morelli, M. Kaufman, R. H. G. A. Kiminami, J. Mater. Sci., 37 (2002) 3569–3572.

28. A. B. Salunkhe, V. M. Khot, M. R. Phadatare, S. H. Pawar, Journal of Alloys and Compounds, 514 (2012) 91–96.
29. Y. Li, J. P. Zhao, J. C. Han, X. D. He, Materials Research Bulletin, 40(6) (2005) 981-989.
30. N. Rezlescu, N. Iftimie, E. Rezlescu, C. Doroftei, P. D. Popa, Sens. Actuators B: Chemical, 114 (2006) 427–432.
31. S. M. Khetre, H. V. Jadhav, P. N. Jagdale, S. V. Bangale, S. R. Bamane, Advances in Applied Science Research, 2(2) (2011) 252-259.
32. C. Doroftel, E. Rezlescu, N. Rezlescu, P. D. Popa, Rom. J. Phys., 51(5–6) (2006) 631–640.
33. R. Sepahvand, R. Mohamadzade, Journal of Sciences, Islamic Republic of Iran, 22(2) (2011) 177-182.
34. K. C. Patil, S. T. Aruna, S. Ekambaram, Curr. Opin. Solid State Mater. Sci., 2 (1997) 158.
35. S. K. Ghosh, A. Prakash, S. Datta, S. K. Roy, D. Basu, Bull. Mater. Sci., 33(1) (2010) 7–16.
36. M. W. Chase, C. A. Davies, J. R. Downey, D. J. Frurip, R. A. McDonald, A. N. Syverud, J. Phys. Chem. Ref. Data, 14(l.1) (1985).
37. F. Rafat, Arch. Appl. Sci. Res., 6(5) (2014) 75-78.
38. J. P. Chen, K. J. Isa, Mass spectrum. Soc. Jpn., 46 (1998) 299-303.
39. S. M. Hoque, M. A. Hakim, A. Mamun, S. Akhter, T. Md. Hasan, D. P. Paul, K. Chattopadhayay, Materials Sciences and Applications, 2 (2011) 1564-1571.
40. J. G. Paik, M. J. Lee, S. H. Hyun, Thermochim. Acta, 425 (2005) 131–136.
41. K. Mukherjee, D. C. Bharti, S. B. Majumder, Sensors and Actuators B 146 (2010) 91–97.
42. A. Alarifi, N. M. Deraz, S. Shaban, J. Alloys Compd., 486 (2009) 501–506.
43. J. Chandradass, A. H. Jadhav, K. H. Kim, H. Kim, Journal of Alloys and Compounds, 517 (2012) 164–169.
44. Y. -S. Cho, Y. -D. Huh, Bull. Korean Chem. Soc., 30(6) (2009) 1413-1415.
45. Z. Wang, P. Lazor, S. K. Saxena, H. S. C. O'Neil, Mater. Res. Bull., 37 (2002) 1589-1594.
46. F. Nakagomi, S. W. Da Silva, V. K. Garg, A. C. Oliveira, P. C. Morais, A. Franco Jr., J. Solid State Chem., 182 (2009) 2423.
47. Z. Ž. Lazarević, Č. Jovalekić, D. Sekulić, M. Slankamenac, M. Romčević, A. Milutinović, N. Ž. Romčević, Science of Sintering, 44 (2012) 331-339.
48. Y. Liu, H. Miyoshi, M. Nakamura, Int. J. Cancer, 120 (2007) 2527–2537.
49. V. Šepelák, I. Bergmanna, D. Menzel, A. Feldhoff, P. Heitjans, F. J. Litterst, K. D. Beckera, J. Magn. Magn. Mater., 316(2) (2010) 764-767.
50. A. Tomitaka, H. Kobayashi, T. Yamada, M. Jeun, S. Bae, Y. Takemura, IEEE (2010)

Садржај: *У овом раду представљени су резултати везани за синтезу нанокомпозитног праха $MgFe_2O_4$ процесом сраљивања из раствора горива који садржи уреу (U) и амонијум ацетат (AA). Утицај смеше горива и температуре синтеровања на формирање фаза, структурна, морфолошка и магнетна својства честица $MgFe_2O_4$ праћена су XRD, TGA, Раманом, SEM, EDAX и VSM анализом. Термодинамичко моделовање реакције сагоревања је показало да се употребом горива које садржи уреу и амонијум ацетат, адијабатска температура пламена (T_{ad}), егзотермност и количина гаса ослобођеног након сагоревања као и својства продуката, могу контролисати. Употребом смеше горива (U и AA) у синтези $MgFe_2O_4$ нађено је да се добијају ферити са финијим агломератима, веће кристалиничности, бољих магнетних*

својстава и мање величине кристалита, него када се употребњава чиста уреа. Само узорци који су припремљени у саставу 0.5U + 0.5AA и синтеровани на 900°C, 2 h праве чист феритни спинел док прахови синтеровани на 600°C, 2 h имају секундарних фаза. Раман спектроскопија је такође потврдила да је $MgFe_2O_4$ феритни спинел, без обзира на друге методе..

Кључне речи: *синтеза сагоревања из раствора; смеша горива; температура синтеровања; термодинамичка анализа; магнетне наночестице*